

Carbon dioxide consumption and bicarbonate production rates by continental weathering at the LGM and at present-day—an update

GUY MUNHOVEN

Bristol Glaciology Centre, School of Geographical Sciences, University of Bristol, University Road, Bristol BS8 1SS, UK

e-mail: g.munhoven@bris.ac.uk

Abstract We construct a range of estimates for the glacial–interglacial variations of CO₂ consumption and HCO₃⁻ production rates by continental weathering processes, using two models of continental weathering in conjunction with two data sets for present-day runoff and climate results from four general circulation models. Both models consistently produce 25–35% higher global CO₂ consumption and 30–40% higher HCO₃⁻ production rates at the Last Glacial Maximum (LGM) than at present-day. In terms of CO₂ consumed by silicate weathering, variations calculated here are more than 2.5 times smaller than those derived from the marine Ge/Si record. Areas exposed both now and at the LGM exhibit only little change. The increased HCO₃⁻ production (CO₂ consumption) on the continental shelf exposed at the LGM overbalances the decrease due to ice cover by a factor of 3–4 (respectively 2.3–3.7). However, large uncertainties affect the fluxes in the shelf environment, as shown by sensitivity tests regarding its lithology.

INTRODUCTION

Earth surface conditions at the Last Glacial Maximum (LGM) were considerably different from those of today. Extensive ice sheets covered large areas of the continents at high latitude. The global sea level stood 120–130 m lower; large extents of the currently flooded continental shelf lay free and were subject to erosion (Fig. 1). The net effect of these changes on chemical weathering in general, and on CO₂ consumption or HCO₃⁻ production rates in particular, is still subject to debate. In their review of chemical weathering over glacial time scales, Kump & Alley (1994) concluded that global chemical weathering rates were comparable during glacials and interglacials. Quantitative reconstructions give, however, very contrasting results, depending on the method they are based on. According to the continental weathering model of Gibbs & Kump (1994), global bicarbonate production was only about 20% higher at the LGM than at present-day. On the basis of the marine Ge/Si record, Munhoven & François (1996) calculated that the rate of CO₂ consumption by silicate weathering alone was about 100–250% higher at the LGM than at present.

The aim of this study is to provide new quantitative insight into the individual effects of the large-scale environmental changes mentioned above on the CO₂ consumption and HCO₃⁻ production rates at the LGM and the present-day. As a

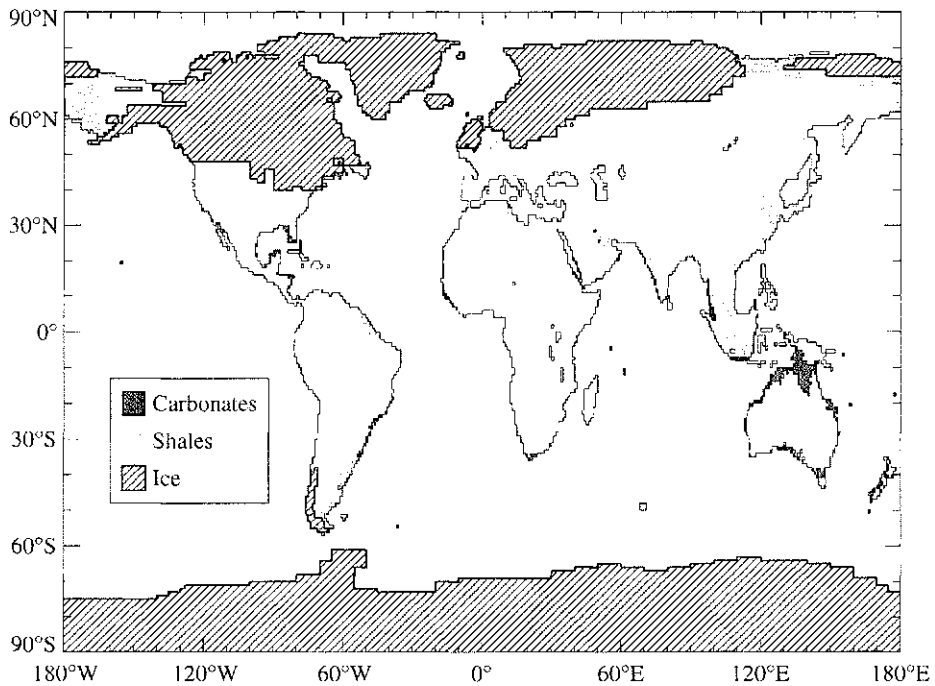


Fig. 1 LGM continental margin lithology and ice sheet extension. The thin lines indicate the continental outlines for the LGM. The hatched areas delimit the ice sheet extent. Dark zones represent shelf areas exposed at LGM but presently flooded, with carbonate outcrops in black and shale outcrops in grey.

starting point, we use the model developed by Gibbs & Kump (1994). By combining two different data sets for present-day runoff with four different General Circulation Model (GCM) climatologies, we generate a set of eight different estimates of the distribution of glacial-to-interglacial runoff variations. This diversity of possible runoff variations provides the opportunity to estimate the uncertainties affecting our results. The significance of our results is further tested by comparing them to those derived from GEM-CO₂ ("Global Erosion Model for CO₂ consumption", Amiotte Suchet & Probst, 1995a,b), a weathering model similar to that of Gibbs & Kump (1994). Finally, we add several sensitivity tests regarding the lithology of the emerged continental margin, which remains a critical unknown.

METHODOLOGY

In this section, we first present a summary description of the two weathering models (Gibbs & Kump, 1994; Amiotte-Suchet & Probst, 1995a,b). We explain how the models are adapted and extended for their application in an LGM environment. Finally, we define the procedures used to calculate the glacial–interglacial variations of the global HCO₃⁻ and CO₂ fluxes.

The weathering models

The two weathering models under consideration have a common structure. Both take a map of global lithology and determine the distribution of bicarbonate produced by chemical weathering from runoff intensity, by using a set of empirical bicarbonate flux–runoff relationships for major rock types. The Gibbs & Kump (1994) weathering model (hereafter GKWM) uses a map with six classes: carbonates, shales, sandstones, extrusive igneous rocks, shields and a “complex” class, for grid-points not clearly fitting into any of the first five classes. The map of GEM-CO₂ differentiates between seven classes (Amiotte-Suchet & Probst, 1995a,b): carbonates, shales, sands and sandstones, plutonic and metamorphic rocks, acid volcanic rocks, basalts, and evaporites. The empirical relationships that link the bicarbonate production rates to runoff intensity in GKWM are taken from Bluth & Kump (1994); those in GEM-CO₂ are from Amiotte Suchet & Probst (1993). Neither GKWM nor GEM-CO₂ allows for weathering beneath ice.

Unfortunately, the lithology map of GEM-CO₂ has not yet been published. At the global scale, only present-day CO₂ and HCO₃⁻ flux distributions have been presented (Amiotte Suchet & Probst, 1995a,b). As detailed below, the information provided by these two distributions is nevertheless sufficient for the purpose of this study.

LGM geography, ice-cover and lithology

In order to apply the models in an LGM environment, appropriate boundary conditions regarding ice-cover, shelf exposure and shelf lithology must be provided.

The ice-sheet extent used with both models is taken from Peltier (1994). The boundaries of the exposed shelf that we use with GEM-CO₂ is also taken from Peltier (1994). The lithology of the grid-points that represent the exposed shelf at the LGM is then defined as follows. Grid-elements around Australia and the Caribbean are considered to consist of carbonate outcrops, except where they are close to large river mouths or to present-day coastal swamp areas. These points, and the remaining ones at high latitude, are considered to consist of shale exposures. The resulting map of the continental margin lithology is represented in Fig. 1. The lithology map of GKWM includes an adequate shelf extension that we use unchanged.

Runoff reconstruction

For each grid element falling on land, the estimated LGM runoff, R_{LGM} , is calculated from its present-day observed value, R_{obs} , by setting $R_{\text{LGM}} = R_{\text{obs}} + \Delta R$. The anomaly relative to present-day, ΔR , is calculated from GCM climatologies, using the difference between the annual average distributions of total precipitation and evaporation ($P - E$) as an estimator for continental runoff. Hence, $\Delta R = (P - E)_{\text{GCM(LGM)}} - (P - E)_{\text{GCM(present)}}$. The subscripts “GCM(LGM)” and “GCM(present)” refer to GCM results from the LGM and the present-day (control) experiments respectively. To avoid physically meaningless negative values for R_{LGM} , ΔR is set equal to its lower bound $-R_{\text{obs}}$ where

necessary. In order to use this approach for the total LGM land area, the observed present-day runoff distribution is first extrapolated to the exposed shelf areas.

Gibbs & Kump (1994) used the UNESCO runoff distribution (Korzoun *et al.*, 1977) for their calculations with GKWM. Amiotte Suchet & Probst (1995a,b) based their flux distributions on the sum of the monthly mean positive values of the $P - E$ distributions published by Willmott *et al.* (1985). There are sensible differences between these two runoff distributions. As they set the lower limit of ΔR (i.e. they set the largest decrease), they also influence our estimates for the glacial–interglacial variations. Both have therefore been considered for this study. The UNESCO runoff distribution is nevertheless replaced by that of the hydrographic database GGHYDRO (Cogley, 1998). This distribution is available in numerical form and is largely derived from the UNESCO one. GGHYDRO furthermore contains other data that we use, such as masks to define internally and externally drained areas.

Publicly available output data sets from four different GCMs are taken into consideration to calculate the ΔR distributions. These models are: CCM0 (Wright *et al.*, 1993; Kutzbach, 1994), CCM1 (Kutzbach *et al.*, 1996, 1998), ECHAM2 (Lautenschlager & Herterich, 1990) and GISS (Overpeck *et al.*, 1989; Rind, 1994). By combining the two runoff and the four GCM data sets, we get eight different estimates for the LGM runoff distribution to be used with the two weathering models.

All of the data sets are first downscaled from their original grids to a $1^\circ \times 1^\circ$ grid. This downscaling is performed by redistribution, without interpolation for the lithology map (GKWM only), and by area-weighted interpolation for the GCM data.

CO₂ and HCO₃⁻ fluxes

The different reconstructions for the LGM runoff can now be used in GKWM and GEM-CO₂ to calculate LGM distributions of HCO₃⁻ production and of CO₂ consumption.

These calculations are obviously straightforward to carry out with GKWM, as all of the required components have been published. It should only be mentioned that the “complex” lithology class is assigned a globally constant composition in terms of the five basic rock types considered in GKWM, as described in Jones *et al.* (1999).

For GEM-CO₂, calculations need to be done indirectly because its lithology map is not yet available. In this model, CO₂ and HCO₃⁻ fluxes are simply proportional to runoff. As a consequence, two flux distributions F and F_0 (both of either CO₂ or HCO₃⁻) that result from two runoff distributions R and R_0 respectively, are related by $F/F_0 = R/R_0$. We can thus calculate F for an arbitrary R from the F_0 distributions published by Amiotte Suchet & Probst (1995a,b), knowing that the runoff distribution R_0 they are based on is derived from the $P - E$ data of Willmott *et al.* (1985). At grid-points where F_0 and R_0 are equal to zero, F is also set to zero. The error on the global fluxes due to this simplification is insignificant. The grid-points at issue represent only 2.4% of the externally drained area, and, in the GGHYDRO runoff distribution, they account for less than 0.2% of the total external runoff.

In order to compare the effects of the different changes such as the extended ice-cover and shelf exposure, the LGM land area is partitioned into four non-overlapping

zones. The individual contribution from each zone in the global variations of the rates of CO_2 consumption and HCO_3^- production is then determined by integrating the LGM-minus-present-day differences of the respective flux distributions over that zone.

Zone LI: presently exposed land that was covered by ice at the LGM At each point in this zone, the presence of ice at the LGM reduced the weathering rates to zero.

Zone LX: presently exposed land that was also exposed at the LGM In this zone, only runoff redistribution may affect global HCO_3^- production and CO_2 consumption rates. Such redistributions may equally well cause higher or lower LGM rates.

Zone SI: presently flooded shelf that was covered by ice at the LGM The impact of the grid-elements in this zone on CO_2 consumption and HCO_3^- production is zero.

Zone SX: presently flooded shelf that was exposed at the LGM This zone of newly exposed land invariably contributed to increase both HCO_3^- production and CO_2 consumption rates at the LGM.

RESULTS AND DISCUSSION

Below, we focus on the fluxes from externally drained areas alone, although some results relative to the total continental area are reported in the tables. Fluxes from externally drained areas are the more important ones in the global carbon cycle, since they link the terrestrial to the oceanic environment.

Present-day fluxes

From data in the literature, we calculate that the total bicarbonate flux from externally drained areas is about $31.9\text{--}35.7 \text{ Tmol year}^{-1}$ ($1 \text{ Tmol} = 10^{12} \text{ mol}$). This estimate is based on an average HCO_3^- concentration of $846 \mu\text{mol l}^{-1}$ (Meybeck, 1979) and a global runoff ranging between $37\,400 \text{ km}^3 \text{ year}^{-1}$ (Meybeck, 1979) and $42\,200 \text{ km}^3 \text{ year}^{-1}$ (calculated from GGHYDRO data). 65–67% of this flux stems from the atmosphere (e.g. Berner & Berner, 1996). In this discussion, we have adopted present-day reference values of $33.8 \text{ Tmol HCO}_3^- \text{ year}^{-1}$ and $22.3 \text{ Tmol CO}_2 \text{ year}^{-1}$ for the two fluxes.

Total HCO_3^- production and CO_2 consumption rates calculated from the two models are reported in Table 1. Both models yield bicarbonate fluxes that are significantly below the observed range: GEM- CO_2 falls short by 15–23% and GKWM by 27–32%. Table 1 also indicates that the partitioning of the total bicarbonate flux into an atmospheric and a crustal part is different for the two models. With GKWM, we find that the atmosphere provides 83–84% of the total bicarbonate production. With GEM- CO_2 , this fraction is 70–71%, in much better agreement with the previously cited estimates from

the literature. These apparently comparable fractions put completely opposite weights on silicate and carbonate weathering. For an atmospheric fraction of 67%, the ratio of the bicarbonate produced by silicate to that produced by carbonate weathering is 34:66, whereas for an atmospheric fraction of 83% it is 66:34. GKWM hence cycles a much larger fraction of CO₂ through silicate weathering than GEM-CO₂.

Table 1 Present-day global HCO₃⁻ production and CO₂ consumption rates (both in 10¹² mol year⁻¹), and fractions of bicarbonate originating from the atmosphere (in %), as calculated from GKWM and GEM-CO₂ in conjunction with the two runoff data sets under consideration.

Weathering model/runoff data set combination	Total continent:			Externally drained only:		
	HCO ₃ ⁻	CO ₂	% atm	HCO ₃ ⁻	CO ₂	% atm
GKWM and GGHYDRO runoff	29.0	24.2	83	24.6	20.6	84
GKWM and Willmott <i>et al.</i> (1985) <i>P - E</i>	28.2	23.2	83	22.8	18.9	83
GEM-CO ₂ and GGHYDRO runoff	30.9	22.0	71	28.7	20.4	71
GEM-CO ₂ (and Willmott <i>et al.</i> , 1985, <i>P - E</i>)	30.9	21.3	69	26.2	18.4	70

Glacial–interglacial variations

Table 2 lists the calculated LGM-minus-present-day variations together with standard deviations for each of the two weathering models and for each group of ΔR estimates separately.

The results follow a consistent pattern for the GCM induced variability. ECHAM2 is in each zone responsible for the lowest variations, i.e. the largest decreases and smallest increases. It is also the only model leading to flux decreases in zone LX. The GISS model always produces the highest increases in this zone and it gives the highest global net response. In zone SX, CCM1 yields the highest increase.

The two runoff data sets do not generally lead to significantly different results, except in zone LI. Here, the data from Cogley (1998) produce consistently larger decreases than the Willmott *et al.* (1985) data, essentially because *P - E* is significantly lower than runoff at high latitudes.

The average variations produced by the two weathering models for each group of ΔR estimates and for each zone agree well in general. GEM-CO₂ may appear to produce generally larger increases than GKWM. The differences between the average responses of the two models are nevertheless within the estimated ranges of uncertainty. It is again only in zone LI where differences between the two models might be significant, with GEM-CO₂ predicting smaller decreases than GKWM.

The three zones produce markedly different effects. The increase in HCO₃⁻ production due to shelf exposure (zone SX) is on average 3–4 times as large as the decrease due to the ice-cover (zone LI). For CO₂ consumption, the corresponding ratio is about 2–4. The average variations in the region exposed both now and at the LGM (zone LX) are in general almost an order of magnitude lower than those in zone SX, and are comparable to the estimated uncertainty of the global net variation.

Both GKWM and GEM-CO₂ consistently predict that the total fluxes of bicarbonate and CO₂ through weathering processes were significantly higher at the

Table 2 LGM-minus-present-day variations of HCO_3^- production and CO_2 consumption rates by continental weathering processes in externally drained areas: (*top*) GKWM; (*bottom*) GEM- CO_2 . The headings LI, LX and SX refer to the respective LGM land zones defined in the text. All figures are given in 10^{12} mol year $^{-1}$ and have been rounded to one decimal before reporting.

Runoff data set	GCM data set	HCO_3^- production rate variation:				CO_2 consumption rate variation:			
		LI	LX	SX	Net	LI	LX	SX	Net
Cogley (1998)	CCM0		+1.9	+12.6	+9.5		+1.2	+7.7	+4.8
	CCM1	-5.0	+0.9	+14.0	+9.9	-4.1	+0.4	+8.8	+5.1
	ECHAM2		-0.8	+11.4	+5.6		-0.9	+7.4	+2.4
	GISS		+3.1	+13.2	+11.3		+2.2	+8.4	+6.5
	Average ($\pm 1s$)	-5.0	+1.3 (± 1.7)	+12.8 (± 1.1)	+9.1 (± 2.4)	-4.1	+0.7 (± 1.3)	+8.1 (± 0.6)	+4.7 (± 1.7)
Willmott <i>et al.</i> (1985) <i>P-E</i>	CCM0		+1.7	+12.7	+11.8		+1.0	+7.4	+5.4
	CCM1	-3.6	+0.8	+14.1	+11.3	-3.0	+0.4	+8.5	+5.9
	ECHAM2		-0.7	+11.6	+7.3		-0.9	+7.1	+3.2
	GISS		+3.0	+13.4	+12.8		+2.2	+8.1	+7.3
	Average ($\pm 1s$)	-3.6	+1.2 (± 1.6)	+13.0 (± 1.1)	+10.5 (± 2.4)	-3.0	+0.7 (± 1.3)	+7.9 (± 0.6)	+5.4 (± 1.7)
Global average variations ($\pm 1s$)		-4.3 (± 0.7)	+1.2 (± 1.5)	+12.9 (± 1.0)	+9.8 (± 2.3)	-3.5 (± 0.6)	+0.7 (± 1.2)	+7.9 (± 0.6)	+5.1 (± 1.6)

Runoff data set	GCM data set	HCO_3^- production rate variation				CO_2 consumption rate variation			
		LI	LX	SX	Net	LI	LX	SX	Net
Cogley (1998)	CCM0		+1.9	+13.6	+11.3		+0.8	+8.8	+6.6
	CCM1	-4.2	+1.3	+16.3	+13.4	-3.0	+0.6	+10.9	+8.5
	ECHAM2		-1.7	+11.4	+5.5		-1.2	+8.2	+4.0
	GISS		+4.3	+14.6	+14.7		+2.7	+9.9	+9.6
	Average ($\pm 1s$)	-4.2	+1.5 (± 2.5)	+14.0 (± 2.0)	+11.2 (± 4.1)	-3.0	+0.8 (± 1.6)	+9.4 (± 1.2)	+7.2 (± 2.4)
Willmott <i>et al.</i> (1985) <i>P-E</i>	CCM0		+2.0	+14.1	+13.2		+0.9	+8.3	+7.2
	CCM1	-2.9	+1.3	+16.6	+15.0	-2.0	+0.7	+10.2	+8.9
	ECHAM2		-1.1	+11.8	+7.8		-0.8	+7.6	+4.8
	GISS		+4.4	+15.0	+16.5		+2.8	+9.3	+10.1
	Average ($\pm 1s$)	-2.9	+1.6 (± 2.3)	+14.4 (± 2.0)	+13.2 (± 3.8)	-2.0	+0.9 (± 1.5)	+8.9 (± 1.1)	+7.8 (± 2.3)
Global average variations ($\pm 1s$)		-3.5 (± 0.7)	+1.6 (± 2.2)	+14.2 (± 1.9)	+12.2 (± 3.8)	-2.5 (± 0.5)	+0.8 (± 1.4)	+9.2 (± 1.1)	+7.5 (± 2.2)

LGM. The typical increases relative to present-day are 30–40% for HCO_3^- and 23–34% for CO_2 ; all of the calculated variations fall into the ranges of 22–50% (HCO_3^-) and 11–45% (CO_2). Our results thus document much larger variations of the total bicarbonate flux than the study of Gibbs & Kump (1994).

The analysis of the results from Table 2 in terms of CO_2 consumed by carbonate and silicate weathering processes yields more contrasting results. For carbonate weathering, GKWM results translate into a 4.7 ± 0.7 Tmol year $^{-1}$ higher CO_2 consumption at the LGM than at present day. With GEM- CO_2 , this increase is 4.7 ± 1.7 Tmol year $^{-1}$ (5.5 ± 0.7 Tmol year $^{-1}$ if the ECHAM2-based runoff estimates are disregarded). For silicate weathering, the GEM- CO_2 results document an LGM-minus-present-day difference of 2.8 ± 1.1 Tmol year $^{-1}$ (hence higher consumption at the LGM). According to the GKWM results, this variation would be

Table 3 Sensitivity of shelf bicarbonate production (in Tmol year⁻¹, i.e. 10¹² mol year⁻¹) at the LGM to the adopted shelf lithology as calculated from the two weathering models.

Runoff data set	GCM data set	Homogeneous sandstone shelves:		Homogeneous shale shelves:		Homogeneous carbonate shelves:	
		GEM-CO ₂	GKWM	GEM-CO ₂	GKWM	GEM-CO ₂	GKWM
Cogley (1998)	CCM0	+1.5	+1.0	+5.9	+7.2	+29.8	+19.1
	CCM1	+1.9	+1.2	+7.7	+8.5	+38.7	+23.3
	ECHAM2	+1.6	+1.0	+6.3	+7.5	+32.1	+19.7
	GISS	+1.8	+1.2	+7.0	+8.3	+35.6	+22.1
	Average (±1s)	+1.7 (±0.2)	+1.1 (±0.1)	+6.7 (±0.8)	+7.9 (±0.6)	+34.1 (±3.9)	+21.0 (±2.0)
Willmott <i>et al.</i> (1985) <i>P - E</i>	CCM0	+1.2	+0.9	+4.9	+6.4	+24.6	+17.0
	CCM1	+1.6	+1.1	+6.4	+7.7	+32.6	+21.0
	ECHAM2	+1.3	+0.9	+5.1	+6.5	+26.0	+17.4
	GISS	+1.5	+1.0	+5.9	+7.5	+29.8	+19.9
	Average (±1s)	+1.4 (±0.2)	+1.0 (±0.1)	+5.6 (±0.7)	+7.0 (±0.7)	+28.3 (±3.6)	+18.8 (±1.9)
Global average variations (±1s)		+1.6 (±0.2)	+1.0 (±0.1)	+6.2 (±0.9)	+7.5 (±0.8)	+31.2 (±4.7)	+19.9 (±2.2)

0.4 ± 1.0 Tmol year⁻¹, which also includes the possibility of a lower consumption rate for the LGM. The most important result here is that even the largest supported increase (3.9 Tmol year⁻¹, equivalent to 36% of the present-day rate) is well below the minimum increase of 95% calculated by Munhoven & François (1996).

Sensitivity tests for shelf lithology

The results of the sensitivity tests on homogeneous shelves, covered only by either sandstone, shale or carbonate outcrops, are reported in Table 3. These results first illustrate the wide range of variability that may affect our estimates of HCO₃⁻ production rates by weathering in this environment. The variability due to the different runoff reconstructions is relatively low. Interestingly, it is the CCM0 rather than the ECHAM2 data that produce the lowest variations here. These tests also provide further insight into the sensitivity of the two weathering models. Differences between the GKWM and GEM-CO₂ results can almost entirely be explained from differences between their bicarbonate flux–runoff relationships. Further understanding will require a systematic comparison of the components of the two weathering models. A larger variety of more recent GCM data sets, coupled with other approaches for deriving glacial–interglacial runoff anomalies than the use of *P - E* distributions, will also help to improve the results.

Acknowledgements I would like to thank P. Amiotte Suchet, C. G. Cogley, J. Kutzbach, M. Lautenschlager, W. Peltier, D. Rind, C. Willmott and their colleagues for making the results of their research publicly available. Without their generosity, this study would not have been possible. Financial support for this work is provided by the UK Natural Environment Research Council through Grant GR3/11080.

REFERENCES

- Amiotte Suchet, P. & Probst, J.-L. (1993) Flux de CO₂ consommé par altération chimique continentale: influences du drainage et de la lithologie. *C. R. Acad. Sci. Paris sér. II*, **317**, 615–622.
- Amiotte Suchet, P. & Probst, J.-L. (1995a) A global model for present-day atmospheric/soil CO₂ consumption by chemical erosion of continental rocks (GEM-CO₂). *Tellus* **47B**, 273–280.
- Amiotte Suchet, P. & Probst, J.-L. (1995b) A global 1 degree by 1 degree distribution of atmospheric/soil CO₂ consumption by continental weathering and of riverine HCO₃⁻ yield. *Data base DB1012, CDLAC, Oak Ridge, Tennessee*.
- Berner, E. K. & Berner, R. A. (1996) *Global Environment: Water, Air, and Geochemical Cycles*. Prentice Hall, Upper Saddle River, New Jersey.
- Bluth, G. J. S. & Kump, L. R. (1994) Lithologic and climatologic controls of river chemistry. *Geochim. Cosmochim. Acta* **58**, 2341–2359.
- Cogley, J. G. (1998) GGHYDRO—Global Hydrographic Data, Release 2.2. *Trent Climate Note 98-1, Trent University, Department of Geography, Peterborough, Ontario, Canada*.
- Gibbs, M. T. & Kump, L. R. (1994) Global chemical erosion during the last glacial maximum and the present: sensitivity to changes in lithology and hydrology. *Paleoceanography* **9**, 529–543.
- Jones, I. W., Munhoven, G. & Tranter, M. (1999) Comparative fluxes of HCO₃⁻ and Si from glaciated and non-glaciated terrain during the last deglaciation. In: *Interactions Between the Cryosphere, Climate and Greenhouse Gases* (ed. by M. Tranter, R. Armstrong, E. Brun, G. Jones, M. Sharp & M. Williams) (Proc. Birmingham Symp., July 1999), 267–272. IAHS Publ. no. 256 (this volume).
- Korzoun, V. I., Sokolov, A. A., Budyko, M. I., Voskresensky, K. P., Kalinin, G. P., Konoplyantsev, A. A., Korotkevich, E. S. & Lvovich, M. I. (1977) *Atlas of World Water Balance*. UNESCO Press, Paris.
- Kump, L. R. & Alley, R. B. (1994) Global chemical weathering on glacial time scales. In: *Material Fluxes on the Surface of the Earth* (ed. by T. M. Usselman), 46–60. NRC, Washington DC.
- Kutzbach, J. (1994) CCM0 General Circulation Model output data set. IGBP PAGES/WDC-A for Paleoclimatology Data Contribution Series #94-025, NOAA/NGDC, Boulder, Colorado.
- Kutzbach, J., Behling, P. & Selin, R. (1996) CCM1 General Circulation Model output data set. IGBP PAGES/WDC-A for Paleoclimatology Data Contribution Series #96-027, NOAA/NGDC, Boulder, Colorado.
- Kutzbach, J. E., Gallimore, R., Harrison, S., Behling, P., Selin R. & Laarif, F. (1998) Climate and biome simulations for the past 21,000 years. *Quat. Sci. Rev.* **17**, 473–506.
- Lautenschlager, M. & Herterich, K. (1990) Atmospheric response to ice age conditions: climatology near the earth's surface. *J. Geophys. Res.* **95**, 22 547–22 557.
- Meybeck, M. (1979) Concentrations des eaux fluviales en éléments majeurs et apports en solution aux océans. *Rev. Géol. Dyn. Géogr. Phys.* **21**, 215–246.
- Munhoven, G. & François, L. M. (1996) Glacial–interglacial variability of atmospheric CO₂ due to changing continental silicate rock weathering: a model study. *J. Geophys. Res.* **101**, 21 423–21 437.
- Overpeck, J. T., Peterson, L. C., Kipp, N., Imbrie, J. & Rind, D. (1989) Climate change in the circum-North Atlantic region during the last deglaciation. *Nature Lond.* **338**, 553–557.
- Peltier, W. R. (1994) Ice age paleotopography. *Science* **265**, 195–201.
- Rind, D. (1994) General Circulation Model output data set. IGBP PAGES/WDC-A for Paleoclimatology Data Contribution Series #94-012, NOAA/NGDC, Boulder, Colorado.
- Willmott, C. J., Rowe, C. M. & Mintz, Y. (1985) Climatology of the terrestrial seasonal water cycle. *J. Clim.* **5**, 589–606.
- Wright, H. E., Kutzbach, J. E., Webb III, T., Ruddiman, W. F., Street-Perrott, F. A. & Bartlein, P. J. (eds) (1993) *Global Climates since the Last Glacial Maximum*. University of Minnesota Press, Minneapolis, Minnesota.